

**Role of subcycle transition dynamics in high-order-harmonic generation in periodic structures**

Peter G. Hawkins\*

*Department of Physics, Imperial College London, South Kensington Campus, SW7 2AZ London, United Kingdom*

Misha Yu. Ivanov

*Max-Born-Institute, Max-Born Strasse 2A, D-12489 Berlin, Germany and**Department of Physics, Imperial College London, South Kensington Campus, SW7 2AZ London, United Kingdom*

(Received 18 February 2013; published 25 June 2013)

In this paper a method is presented for calculating the subcycle rate for transitions of electrons between two bands of a sinusoidal band structure. A simple closed-form expression for the rate is derived. We show that transition dynamics are sensitive to the shape of the band structure away from the minima of the conduction band. A model of high-order-harmonic generation in periodic solids that incorporates the subcycle dynamics of transitions across the band gap is described. Harmonic emission is found to be highly sensitive to the temporal shape of the transition rate. Destructive interference of electron currents in the conduction band due to subcycle transition dynamics is described.

DOI: [10.1103/PhysRevA.87.063842](https://doi.org/10.1103/PhysRevA.87.063842)

PACS number(s): 42.65.Ky, 72.20.Ht, 78.47.J–

**I. INTRODUCTION**

Strong-field ionization, pioneered by Keldysh [1], is the first step in processes such as high-order-harmonic generation (HHG). HHG today provides not only a path to the creation of ultrashort light pulses, but also a method for understanding the dynamics of quantum systems. By using HHG in atomic and molecular systems, theory and experiment have come together to explore orbital tomography (see, for instance, [2] and references therein), molecular vibrational and dissociative dynamics [3,4], attosecond hole dynamics [5–8], and many other interesting effects.

Recent experiments by Ghimire *et al.* [9], made possible by lasers operating in the mid-infrared (MIR) range, have shown that it is also possible to generate nonperturbative high-order harmonics within periodic solid structures. There is hope that HHG in solids may be used to understand carrier dynamics [10], and how the laser field affects the band structure, on a subcycle time scale. There have been several approaches to theoretically analyze the generation of high-order harmonics in periodic solids [11–16].

The first experimental and theoretical studies of subfemtosecond currents in dielectrics have recently been carried out [17,18]. The experiments measured the dependence of the current induced in a dielectric on the carrier-envelope phase of the nearly-single-cycle driving pulse [17]. The theoretical analysis developed in [17,18] uses the basis of localized Wannier-Stark states and the concept of Zener tunneling to interpret the experimental results [17]. Quantum beats occurring in dielectrics exposed to few-cycle laser pulses have been theoretically studied in Ref. [19]. The authors of [19] note that although Ref. [1] provides cycle-averaged transition rates, a description on the subcycle time scale is missing. Here we provide a very simple method to obtain this missing information. We work in the basis of delocalized Bloch states rather than in the basis of localized Wannier-Stark states used

in [17,18]. The results are applied to the description of high harmonic emission driven by mid-IR fields [9].

Within the model of [15] the number density of electrons in the band is time independent. The key step in decoding time-resolved information encoded in any nonlinear spectroscopy, such as high-order-harmonic emission, is the development of analytical models capturing the essence of the process. In this context, a description of the subcycle dynamics of the transitions across the band gap is the key first step.

Transitions between bands of states of periodic solids were considered by Keldysh in the second half of his seminal paper on ionization [1]. Keldysh found that in the low-frequency limit the transition rate took a form very similar to that of the tunneling rate in atoms. Gruzdev developed the work of Keldysh by applying it to cosine band structures [20] to obtain a (time-averaged) transition rate and notes that the band structure plays an important role in determining the rate, as we find in this work also.

We show that in typical experimental conditions of [9] the transition dynamics are sensitive to large values of quasimomentum away from the minima of the conduction band. The sensitivity arises not due to electron acceleration after transition to the conduction band, but during the transition itself. Small changes in the band structure due to interactions beyond the nearest-neighbor approximation can be exponentially enhanced; see Sec. IV.

Given that transitions across the band gap are similar to nonadiabatic tunneling we present a strong-field approach, similar to that of [21], to describe the subcycle transition dynamics of electrons in periodic solids. We note here that transitions across the band gap have a nature that is comprised of both tunneling and multiphoton schemes, and as such we shall refer to them simply as transitions. In Sec. II we present the method by which the transition rate is calculated for a band structure typical of the tight-binding approximation. In Sec. III the strong-field, low-frequency limit of the transition rate is discussed and a closed-form analytic approximation to the transition rate is derived. A model of HHG in periodic solids that incorporates the subcycle transition dynamics is described in Sec. V.

\*peter.hawkins08@imperial.ac.uk

## II. SUBCYCLE TRANSITION DYNAMICS ACROSS THE BAND GAP

Consider the dispersion band in a bulk solid with nearest-neighbor interactions; the band of states can be approximated as

$$E(q) = E_g + \varepsilon(q), \quad (1)$$

$$\varepsilon(q) = \Delta [1 - \cos(qd)], \quad (2)$$

where  $2\Delta$  is the width of the band,  $d$  is the lattice constant, and  $q$  is the quasimomentum. This sort of band structure may be obtained, for example, from the tight-binding approximation. This particular form has been chosen in line with the band structure used by Ghimire *et al.* [15] to model HHG in ZnO. The parameter  $\Delta$  can be adjusted to incorporate a tight-binding valence band, thereby giving a general description of the band structure. However, in our calculations we use  $\Delta$  for the conduction band, equivalent to assuming infinite effective mass in the valence band. Longer-range terms within (2) (containing cosines of multiples of  $qd$ ) may be important, as has been noted in [15].

In the Lewenstein *et al.* paper [22] the amplitudes of continuum states excited by an electric field from a ground state are calculated. The same approach is used here; it is noted that the continuum states will now take the form of Bloch states. The dipole transition matrix elements (DTMEs) between Bloch states are similar to those between plane waves, and so the derivation of the amplitudes of the continuum states remains much the same as in [22].

The amplitude of creating an electron-hole pair with quasimomentum  $q$  at time  $t$  is denoted by  $b_q(t)$  and is the solution of the equation

$$\dot{b}_q(t) = -i \left( \frac{q^2}{2} + I_p \right) b_q(t) + id(q)E(t) + E(t) \frac{\partial b_q(t)}{\partial q}. \quad (3)$$

Here  $E$  denotes the electric field,  $I_p$  is the ionization potential, and  $d(q)$  is the DTME for quasimomentum  $q$ . This equation is derived under the approximation that the ground state is only weakly depleted. If we make a similar approximation for the case of a periodic solid, that the valence band is only weakly depleted, the semiconductor optical Bloch equations [12] can be written as

$$\dot{p}_q(t) = -i[\varepsilon(q) + E_g]p_q(t) + id(q)E(t) + E(t) \frac{\partial p_q(t)}{\partial q}. \quad (4)$$

Here  $p_q(t)$  is the polarization between the bands and is effectively the probability amplitude of a transition from valence to conduction band at quasimomentum  $q$  and time  $t$ , and is therefore equivalent to  $b_q(t)$ .

The only difference between (3) and (4) is the energy gap that needs to be overcome ( $E_g$  vs  $I_p$ ) and the dispersion of the states the electrons move to [ $q^2/2$  vs  $\varepsilon(q)$ ]. This shows that one can calculate a subcycle transition rate between two bands of a solid in much the same way as between a ground state of an atom and plane-wave states. The solution to (4) can be written

$$b_q(t) = -i \int_0^t dt' E(t') d_x [q - A(t) + A(t')] \times e^{-i \int_{t'}^t dt'' [\Delta(1 - \cos\{d[q - A(t) + A(t'')]\}) + E_g]}. \quad (5)$$

$A$  denotes the vector potential associated with  $E$ .  $q$  is the instantaneous quasimomentum, associated with the canonical momentum  $p$  as  $q(t) = p + A(t)$ . In terms of  $p$  (5) can be rewritten as

$$c_p(t) = -i \int_0^t dt' E(t') d_x [p + A(t')] \times e^{-i \int_{t'}^t dt'' [\Delta(1 - \cos\{d[p + A(t'')]\}) + E_g]}. \quad (6)$$

where  $c_p(t)$  is the amplitude needed to have canonical momentum  $p$  at time  $t$ .

The population of electrons in the conduction band is given [21] by

$$W(t) = \int |b_q(t)|^2 dq. \quad (7)$$

In order to calculate the rate of appearance of electrons in the conduction band, (7) is used in conjunction with many of the ideas used in the calculation of ionization rates for atoms in [21].

From (5) it is easily seen that  $b(t) \propto \int e^{-iS_q(t)}$ , where  $S_q(t)$  is given by

$$S_q(t) = \int_{t'}^t dt'' [\Delta(1 - \cos\{d[q - A(t) + A(t'')]\}) + E_g]. \quad (8)$$

We evaluate  $b_q(t)$  at the saddle point, where the derivative of  $S_q(t)$  is zero. Taking the saddle-point equation gives us an equation for the times of ionization,  $t'$ , for any pair of  $q$  and  $t$ :

$$\Delta(1 - \cos\{d[q - A(t) + A(t')]\}) + E_g = 0. \quad (9)$$

In terms of  $p$  (9) is

$$\Delta(1 - \cos\{d[p + A(t')]\}) + E_g = 0. \quad (10)$$

Equation (9) can be rearranged into the form

$$d[q - A(t) + A(t')] = i \cosh^{-1} \left( 1 + \frac{E_g}{\Delta} \right). \quad (11)$$

If we set  $E_g = 0$  (similar to setting  $I_p$  to 0 in the atomic case) we see that (11) recovers the classical picture describing an electron being excited at  $t'$  and reaching momentum  $q$  by time  $t$ . This suggests that, since we are dealing with transitions to states near the minima of the conduction band, we can set the momentum just after the transition,  $q$ , to zero. This approximation is equivalent to parametrizing  $p$  as  $p = -A(t)$  with  $t$  acquiring the meaning of the ‘‘birth time’’ for classical two-step models of ionization. This is a reasonable approximation near the peaks of the field, but not near the zeros. In any case, if we are interested in subcycle dynamics we can use an approximation similar to that used for the case of atoms: for low-frequency fields the transition rate is dominated by low initial momenta.

It can also be seen from (11) that  $t'$  must be complex. Taking these points into account we arrive at

$$\sin(\omega t) - \sin(\omega t') = -i \left[ \frac{dE_0}{\omega} \right]^{-1} \cosh^{-1} \left( 1 + \frac{E_g}{\Delta} \right). \quad (12)$$

Here we have neglected the change in the envelope of the laser pulse during a cycle, for the purpose of extracting an analytic solution.

Equation (12) is of the form

$$\sin(\omega t') = \alpha + i\beta. \quad (13)$$

Here  $\alpha$  and  $\beta$  are defined by

$$\alpha = \sin(\omega t), \quad (14)$$

$$\beta = \frac{1}{\mu} \cosh^{-1} \left( 1 + \frac{E_g}{\Delta} \right), \quad (15)$$

and we have denoted  $\mu = dE_0/\omega$ . This is an important parameter that is equivalent to the Bloch frequency of the band divided by the field's frequency. If it is greater than  $\pi$ , then reflections will occur at the band edge. In strong MIR fields  $\mu \gg 1$  and hence  $\beta \ll 1$ .

Continuing with the derivation, since  $t'$  is complex let us write it as

$$t' = t_0 + i\tau; \quad (16)$$

then the solution to (13) is

$$\sin(\omega t_0) = \sqrt{\left(\frac{\tilde{\alpha}^2 + 1}{2}\right) - \sqrt{\left(\frac{\tilde{\alpha}^2 + 1}{2}\right)^2 - \alpha^2}}, \quad (17)$$

$$\sinh(\omega\tau) = \sqrt{\left(\frac{\tilde{\alpha}^2 - 1}{2}\right) + \sqrt{\left(\frac{\tilde{\alpha}^2 - 1}{2}\right)^2 + \beta^2}}, \quad (18)$$

where  $\tilde{\alpha}^2 = \alpha^2 + \beta^2$ . Note that the signs of the square roots are chosen such that  $t_0$  is close to  $t$  as we expect transition to occur mostly over imaginary time, similar to gas-phase ionization in this respect.

We also note that  $\alpha$  is related to the canonical momentum  $p$  by the relation  $p = E_0\alpha/\omega$ . This relates the real and imaginary parts of the transition time to the final quasimomentum  $p$ .

We are interested in the rate of electrons appearing in the conduction band at any moment  $t$ , and with  $q = 0$ . Noting the similarities with the case of atomic ionization [21], one finds

$$\Gamma(t) \sim e^{-2\text{Im}[S_0(t)]}. \quad (19)$$

Here  $S_0 = \text{Re}(S_0) - i\text{Im}(S_0)$  denotes the semiclassical action (8) for electrons appearing with  $q = 0$ . This is precisely the case that we have considered above. Finding the saddle-point ionization time (17), (18) and substituting into (8), we obtain the transition rate. This calculation is done analytically in the low-frequency limit in Sec. III.

While the above transition rate has only exponential accuracy, it is already sufficient for calculating the high-order-harmonic spectrum and assessing the role of the transition dynamics on the subcycle time scale. Importantly, it allows us to assess the role of interference of electron currents due to transitions at different phases of the driving laser field.

However, when needed, one can also use the standard recipe, originally proposed by Keldysh [1] to obtain the preexponential factor in Eq. (19). For instance, this would be important for quantitative calculation of the current induced by a femtosecond pulse, as in Refs. [17,19]. The Keldysh recipe is to take the limit of a small frequency, normalizing the transition rate at the maximum of the field to the static tunneling rate. In the case of atoms and molecules, this procedure leads to quantitatively accurate results for both small and large values

of the Keldysh parameter. It introduces two preexponential factors, described in detail in [23]. The first concerns the field-strength dependence proportional to  $E_0^{-2/\sqrt{2E_g}}$ . The second deals with the wave-function geometry in the unit cell. Normalization can also be done with respect to the more elaborate approach developed by Stockman and co-workers [17,18], which is itself calibrated against experiments [17,18].

The calculation of the saddle-point transition times was performed for the case of a continuous field, but can also be calculated numerically for the case of very short pulses where the envelope changes during the half cycle.

One can also express the rate in terms of the final momentum after the end of the pulse; to do so the action is written as

$$S_0(p) = \int_{t'(p)}^t dt'' [\Delta(1 - \cos\{d[p + A(t'')]\}) + E_g]. \quad (20)$$

It follows that the rate is given by

$$\Gamma(p) \sim e^{-2\text{Im}[S_0(p)]}. \quad (21)$$

### III. STRONG-FIELD LOW-FREQUENCY LIMIT

Now we consider the parameter  $\mu$ ; this is equivalent to the ratio of the Bloch frequency to the driving laser frequency  $\omega_b/\omega$ . If this parameter is greater than  $\pi$  then Bragg reflections will occur at the band edge. We find this parameter to be important throughout the rest of this analysis, and we consider the case when this parameter is large,  $\mu \gg 1$ , i.e., for strong or low-frequency fields.

The imaginary part of the semiclassical action results from integration over imaginary time only. The integration variable is written  $t'' = t_0 + i\xi$ . The approximation  $t_0 \approx t$  is made, which is valid near the peaks for the field where most transitions occur. Then  $S_0$  is given by

$$S_0(t) = -i \int_0^\tau d\xi (\Delta\{1 - \cos[\mu h(t, \xi)]\} + E_g). \quad (22)$$

Here  $h(t, \xi)$  is

$$h(t, \xi) = \sin(\omega t)[1 - \cosh(\omega\xi)] - i \cos(\omega t) \sinh(\omega\xi). \quad (23)$$

Over the integration, in the low-frequency limit,  $\cosh(\omega\xi)$  remains close to 1 so that we may write

$$S_0(t) = -i(E_g + \Delta)\tau + i\Delta \int_0^\tau d\xi \cosh[\mu \cos(\omega t) \sinh(\omega\xi)]. \quad (24)$$

Writing  $y = \sinh(\omega\xi)$  and defining

$$a(t) = \mu \cos(\omega t), \quad (25)$$

Eq. (24) becomes

$$S_0(t) = -i(E_g + \Delta)\tau + i\frac{\Delta}{\omega} \int_0^{\sinh(\omega\tau)} dy \frac{\cosh[ay]}{\sqrt{1+y^2}}. \quad (26)$$

In the low-frequency limit  $y^2 < 1$  over the integration and so the binomial expansion  $(1+y^2)^{-1/2} \approx 1 - y^2/2$  is used to arrive at

$$S_0(t) = -i \left[ (E_g + \Delta)\tau - \frac{\Delta}{\omega} f(a(t), \tau(t)) \right], \quad (27)$$

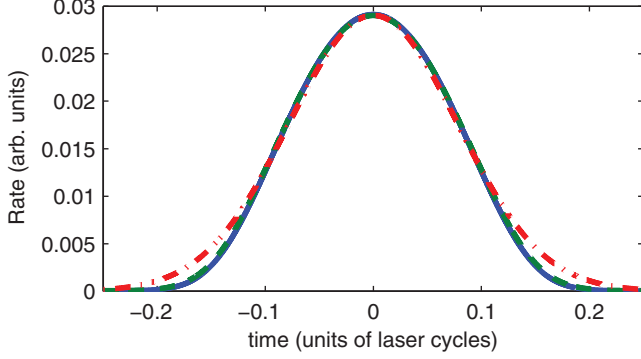


FIG. 1. (Color online) This plot presents a comparison of the transition rate calculated using (24) (blue solid), the approximation of the rate using (27) (green dashed), and a Gaussian approximation (red dot-dashed). The parameters used are those expected for a ZnO experiment. The material properties are  $E_g = 0.125$  a.u. (3.4 eV),  $\Delta = 0.092$  a.u. (2.5 eV), and  $d = 5.29$  a.u. (0.28 nm), which can be seen from [15,24]. The light is characterized by  $\omega = 0.014$  a.u. ( $\lambda = 3.25 \mu\text{m}$ ), and  $\mu = 5$  in line with the work of [9].

where the function  $f$  is given by

$$f(a, \tau) = \frac{\sinh[a \sinh(\omega\tau)]}{a} - \frac{\sinh^2(\omega\tau) \sinh[a \sinh(\omega\tau)]}{2a} + \frac{\sinh(\omega\tau) \cosh[a \sinh(\omega\tau)]}{a^2} - \frac{\sinh[a \sinh(\omega\tau)]}{a^3}. \quad (28)$$

The rate  $\Gamma(t)$  of particles entering the conduction band at time  $t$  given in (19) can then be written out with  $S_0$  given by (27) with  $f$  approximated as in (28).

As discussed in Sec. II one can also express  $t_0$  and  $\tau$  as functions of the canonical momentum  $p$ . This is useful because, as  $\omega t$  approaches  $\pm\pi/2$ , i.e., the edge of the ionization burst, the approximation  $t_0 \approx t$  no longer holds. At these times one has to use  $a[t_0(p)]$  rather than  $a(t)$  (25) with the corresponding change in  $\Gamma(t) \rightarrow \Gamma[t_0(p)]$ .

A comparison of the full calculation of  $\Gamma$  and the approximation given above is given in Fig. 1. One can see that the shape of the fully calculated rate agrees closely with the approximation. A Gaussian fit is also plotted; it does not fit as well toward the minima of the field. The parameters used in the calculation are those expected for a ZnO experiment as described in [15] and are given in the caption.

#### IV. ROLE OF THE BAND STRUCTURE

The parameter written here as  $\beta$  is found to be equivalent to the Keldysh parameter in the case of solids, which he arrives at in the second half of his seminal 1965 paper [1]. In that case a different band structure was used, which is of the form

$$E(q) = E_g \left[ 1 + \frac{\Delta}{E_g} (qd)^2 \right]^{1/2}, \quad (29)$$

corresponding to

$$\varepsilon(q) = E_g \left[ 1 + \frac{\Delta}{E_g} (qd)^2 \right]^{1/2} - E_g. \quad (30)$$

This expression for  $\varepsilon(q)$  should be compared with (2). For small  $q$  ( $qd \ll 1$ ) the two bands are identical,  $\varepsilon(q) \approx \Delta/2(qd)^2$ . Analysis of the saddle-point condition considered above, for the case of the band structure (30), gives the following:

$$\sin(\omega t) - \sin(\omega t') = i \frac{1}{\mu} \sqrt{\frac{E_g}{\Delta}}. \quad (31)$$

Comparison of (31) with (12) shows that the  $\beta$  parameter (15) for the case of Keldysh's band structure is given by

$$\beta_{\text{Keldysh}} = \frac{1}{\mu} \sqrt{\frac{E_g}{\Delta}}, \quad (32)$$

If one considers how the parameters are labeled in this approach compared to that of Keldysh, it is easily verified that  $\beta_{\text{Keldysh}}$  is equivalent to the Keldysh parameter for solids arrived at in [1] (noting that  $\Delta = 1/md^2$  with  $m$  being the reduced mass of the electron-hole pair). The band structure used by Keldysh is an approximation to the band structure around the minima of the band, the region the electron tunnels to. However, during the imaginary tunneling time both the action and thereby the transition rate are sensitive to the shape of the band structure away from the minima of the band. Consider the expression given for the action in (22). The argument of the cosine in (22) is  $\mu h(t, \xi)$  (23); it tells us where the electron is in the conduction band. The maximal value of  $\mu h(t, \xi)$  is at  $\xi = \tau$  and is given by

$$\mu \sinh \left[ \frac{1}{\mu} \cosh^{-1} \left( 1 + \frac{E_g}{\Delta} \right) \right] \approx \cosh^{-1} \left( 1 + \frac{E_g}{\Delta} \right). \quad (33)$$

For typical experimental conditions (given in the caption of Fig. 1) this value is 1.52; thus the shape of the band structure away from the minima is of importance.

If one includes interactions beyond nearest-neighbor terms in the band structure, with a conduction-band dispersion (with  $a, b$  being constants)

$$\varepsilon(q) = \Delta [1 - a \cos(qd) - b \cos(3qd)], \quad (34)$$

then neither the band structure used by Keldysh nor the nearest-neighbor approximation will provide a close fit to the full expression. However, the ability to write a closed-form expression for the transition rate makes a nearest-neighbor model an attractive one.

A plot comparing numerical simulations of the transition rate for nearest-neighbor, Keldysh, and full band structures is shown in Fig. 2. The ionization times were calculated numerically for the full band structure as the solution for the nearest-neighbor band structure cannot be used as an approximation, since small changes can dramatically affect the rate.

From Fig. 2 it is clear that the inclusion of terms beyond the nearest-neighbor approximation can have a dramatic effect on the rate. The inclusion of a  $\cos(3qd)$  term in the band structure stops the band shape matching the nearest-neighbor model in the low- $qd$  range. If one alters the width of the band to be  $\tilde{\Delta} = \Delta/(a + 9b)$  then the band's shapes match for low  $qd$ . In the case of this scaling any differences in the rate are due only to the structure of the band away from the minima. The rate for this band structure with modified bandwidth is also plotted in

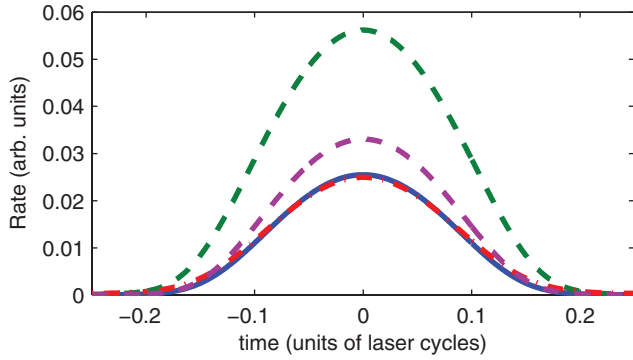


FIG. 2. (Color online) This plot presents a comparison of the transition rate calculated for different band structures. The nearest-neighbor model (2) (blue solid), including a  $3qd$  term [ $a = 0.95$ ,  $b = 0.05$  in (34)] (green dashed), the  $3qd$  model with  $\Delta$  modified so the bands shape matches the other bands in the low- $qd$  range (purple, dashed), and the band structure used by Keldysh (red dot-dashed). The parameters used are those expected for a ZnO experiment, listed in the caption of Fig. 1.

Fig. 2; the rate is then closer to matching the nearest-neighbor model but is still very different.

Even though the nearest-neighbor model and that of Keldysh have a similar magnitude the shape differs. Looking ahead, the calculation of harmonic spectra from solids involves Fourier transforms of the transition rate. Small changes in the shape of the rate could have a large impact on the high-energy part of the harmonic spectrum.

## V. HIGH-ORDER-HARMONIC GENERATION

Electrons that are promoted into the conduction band will move in this band, driven by the same field that caused the transition. The quasimomentum of an electron is given by  $\dot{q} = -E(t)$ , with the initial condition that the electron appeared in the conduction band at a time  $t_a$  with  $q(t_a) = 0$ . The quasimomentum in a continuous electric field is given by

$$q(t) = -\frac{\mu}{d} [\sin(\omega t) - \sin(\omega t_a)]. \quad (35)$$

The group velocity of electrons, given by  $\partial\varepsilon/\partial q$ , with this quasimomentum in a nearest-neighbor band structure is

$$v_g(t, t_a) = -\Delta d \sin[\mu \sin(\omega t) - \mu \sin(\omega t_a)]. \quad (36)$$

The motion of electrons with the group velocity given above leads to an electron current in the conduction band. From Maxwell's equations it is seen that a current  $j(t)$  leads to the creation of an electric field, with the emission intensity proportional to  $|\Omega J(\Omega)|^2$ ; see, e.g., [12]. Here  $J(\Omega)$  is the Fourier transform of the current, and we note that  $\Omega J(\Omega)$  is simply the Fourier transform of  $\partial j/\partial t$ . Calculation of  $\partial j/\partial t$  and its Fourier transform allows a description of the HHG process.

The current is written as

$$j(t) = -\int^t \Gamma(t_a) v_g(t, t_a) dt_a; \quad (37)$$

in this way all electrons previously promoted to the conduction band contribute to the current. In order to calculate the intensity

of harmonics emitted due to this current we take the time differential:

$$\partial j/\partial t = \int^t \Gamma(t_a) \frac{\partial v_g(t, t_a)}{\partial t} dt_a, \quad (38)$$

which yields

$$\partial j/\partial t = -\Delta d \omega \mu \cos(\omega t) \sum_{i=1}^3 G_{i,n}(t), \quad (39)$$

where, for the case of a continuous electric field in which  $N$  half cycles have already occurred, the functions  $G_i(t)$  are

$$G_1(t) = N C(t) \int_{-\pi/2\omega}^{\pi/2\omega} \Gamma(t_a) C(t_a) dt_a, \quad (40)$$

$$G_2(t) = C(t) \int_{-\pi/2\omega}^t \Gamma(t_a) C(t_a) dt_a, \quad (41)$$

$$G_3(t) = S(t) \int_{-\pi/2\omega}^t \Gamma(t_a) S(t_a) dt_a, \quad (42)$$

and

$$C(t) = \cos[\mu \sin(\omega t)], \quad (43)$$

$$S(t) = \sin[\mu \sin(\omega t)]. \quad (44)$$

Here  $G_1$  describes the contribution from the electrons promoted to the conduction band during the previous  $N$  half cycles. The functions  $G_{2,3}$  describe the contributions from the electrons promoted to the conduction band during the half cycle under consideration. Compared to high-order-harmonic emission in atomic or molecular gases, the first term can be associated with the “very long” trajectories, which usually do not make substantial contribution to atomic HHG.

Here, however, the situation seems different. Initially, one may expect that the contributions due to previous half cycles (40) of the field will dominate over the subcycle terms (41), (42), particularly if many half cycles have occurred. It is then tempting to treat the transitions as occurring only at the peaks of the field. Then the integral in (40) simply becomes the number of electrons appearing in each half cycle. Under these approximations  $\partial j/\partial t$  becomes

$$\partial j/\partial t = -\Delta d \omega \mu \cos(\omega t) N(t) C(t) \quad (45)$$

and is analogous to the expression in [15], with  $N(t)$  the number of previous half cycles. However, we find that this initial expectation and the associated approximation are not, in fact, accurate. Physically, in the strong-field limit, the subcycle dynamics of the transitions leads to Bragg reflections at different phases of the field and possible cancellation of currents originating from different phases of the interband transitions. This physical picture is discussed in more detail in the following section.

Mathematically, one can use the Jacobi-Anger expansion of the trigonometric function appearing in (40). Then one finds that the integral is a weighted sum of many Fourier transforms of the transition rate. As a result, the contribution due to previous half cycles is highly dependent on the temporal shape of the transition rate.

This point is illustrated in Fig. 3, where the integral in Eq.(40), denoted  $I(E_0, \lambda)$ , is shown as a function of the

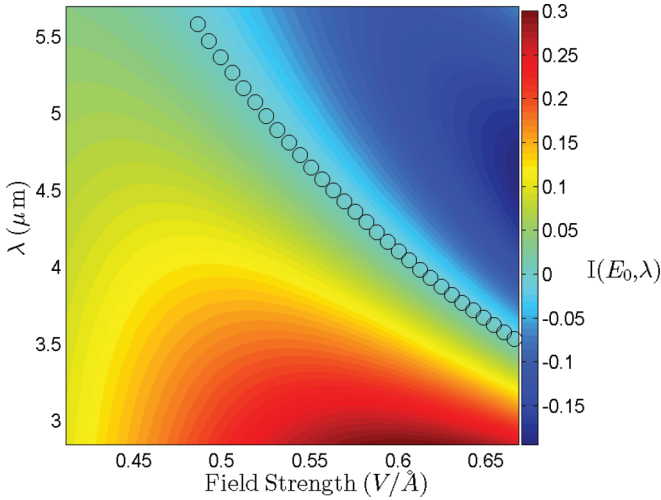


FIG. 3. (Color online) Plot of  $I(E_0, \lambda)$ . All other parameters are those expected for a ZnO experiment, as listed in the caption of Fig. 1. The circular markers lie on the line where  $I(E_0, \lambda)$  is zero, so that contributions to  $\partial j/\partial t$  from previous half cycles do not affect the harmonic spectrum.

laser parameters, for the example of the nearest-neighbor band structure. One can drastically alter the value of  $I(E_0, \lambda)$  by tuning the field strength  $E_0$  and the driving laser wavelength  $\lambda$ .

In particular, one can suppress the effect of previous half cycle contributions by selecting the appropriate laser field strength and wavelength combination (marked with dots in Fig. 3). In this case, only the subcycle effects will be present in the spectrum, very much in contrast with the model of (45). This statement is illustrated in Fig. 4, which shows the time dependence of  $\partial j/\partial t$  for the laser parameters chosen along the lines marked with circles in Fig. 3. We see that the signal does not grow from one laser cycle to the next, as opposed to the model where the current is proportional to the total number of the electrons promoted to the conduction band.

#### A. Destructive interference of electron currents

A physical understanding of how currents created during previous half cycles do not persist at later times is easily obtained. Considering the shape of the integrand in  $I(E_0, \lambda)$ , we see that it has a maximum at  $\sin(\omega t_a) = 0$ ,  $p = 0$  and

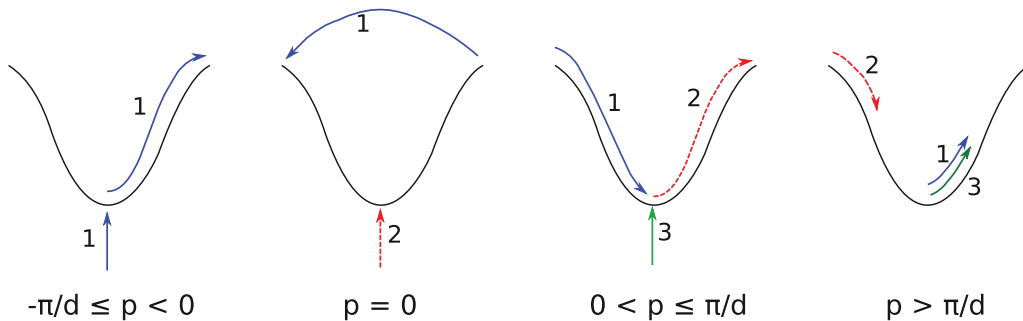


FIG. 5. (Color online) A simplified picture of transition dynamics during a half cycle of the laser field. Three bursts of transition occur; the numbers of electrons in the first and third bursts sum to the the number of electrons in the second burst then currents due to these electrons will interfere destructively.

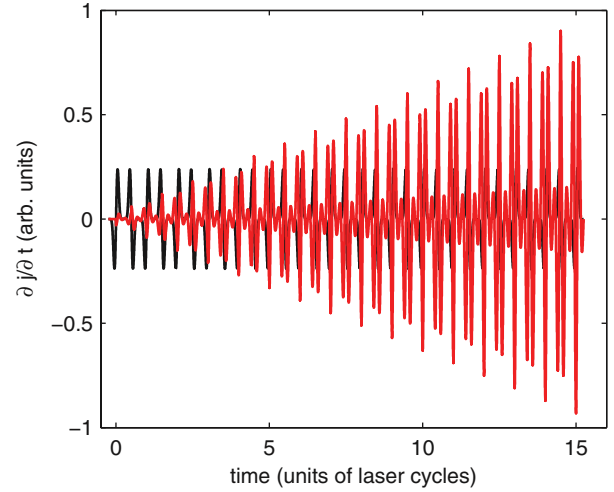


FIG. 4. (Color online) Plot of  $\partial j/\partial t$  for the Ghimire model (red) and our model (black); the laser parameters are  $\lambda = 4.1 \mu\text{m}$  and  $E_0 = 0.6 \text{ V/\AA}$  which correspond with a point on the line in Fig. 3. All other parameters are those expected for a ZnO experiment, as listed in the caption of Fig. 1. The different temporal structures show the importance of the subcycle dynamics for the generated electron currents.

minima at  $\sin(\omega t_a) = \pm\pi/\mu$ ,  $p = \pm\pi/d$ . Here we have used the relationship  $p = (E_0/\omega) \sin(\omega t_a)$  between the transition times  $t_a$  and the associated canonical momenta  $p$ . Maxima and minima beyond these are small enough, for the values of  $\mu$  achievable, to be neglected in this simple analysis.

Thus, there are three prominent instants in time that maximally affect the rate of change of current. Let us assume that transitions occur only at these three times. The value of the group velocity for these three transitions sheds some light on what it means physically for the integral to go to zero. The group velocities at a later time  $t$  due to these three transitions are

$$v_g(t, p = -(\pi/d)) \sim N_1 \Delta d \sin[\mu \sin(\omega t)], \quad (46)$$

$$v_g(t, p = 0) \sim -N_2 \Delta d \sin[\mu \sin(\omega t)], \quad (47)$$

$$v_g(t, p = (\pi/d)) \sim N_3 \Delta d \sin[\mu \sin(\omega t)]. \quad (48)$$

Here  $N_1$ ,  $N_2$ , and  $N_3$  relate to the number of electrons that undergo these transitions. Due to the symmetry of the transition rate  $N_1 = N_3$ . If  $2N_1 = N_2$ , then electron bunches that make transitions at these times will cause currents that cancel one another out after the half cycle. This condition can be satisfied by changing the shape of  $\Gamma$ , i.e., by altering the laser field strength and wavelength, as in Fig. 3. A diagram of the simplified three-burst model is shown in Fig. 5. Note that the last burst appears at the bottom of the conduction band when the first burst returns there; from then on they move together, out of phase with the middle burst.

## VI. CONCLUSIONS

Recent experiments [9] have shown that it is possible to generate nonperturbative high-order harmonics in bulk periodic solids. In order to describe the process of high-order-harmonic emission by an intraband current model, one should consider the subcycle transition dynamics of electrons in the periodic structure.

We have shown that in the low-frequency limit an analytic approximation for the transition rate may be used to describe this dynamics, and that it is sensitive to the shape of the band structure not only near the bottom of the Brillouin zone, but also relatively far away from it. Terms of higher order than the nearest-neighbor interactions in the band structure affect the rate, and thus they may be important for subsequent dynamics [9].

The incorporation of the subcycle transition rate derived in this paper with an intraband current model of HHG from periodic bulk media has been developed. We have shown that the harmonic spectrum is sensitive to the shape of the subcycle structure of the transition rate. The choice of certain laser parameters gives rise to an effect that removes contributions to  $\partial j/\partial t$  from previous half cycles. This cancellation of electron currents is described by a simple three-burst model.

## ACKNOWLEDGMENT

These studies were supported by EPSRC program Grant No. EP/I032517/1.

- 
- [1] L. V. Keldysh, Zh. eksp. teor. Fiz. **47**, 1945 (1964) [Sov. Phys. JETP **20**, 1307 (1965)].
  - [2] P. Salières, A. Maquet, S. Haessler, J. Caillat, and R. Taïeb, *Rep. Prog. Phys.* **75**, 062401 (2012).
  - [3] W. Li, X. Zhou, R. Lock, S. Patchkovskii, A. Stolow, H. C. Kapteyn, and M. M. Murnane, *Science* **322**, 1207 (2008).
  - [4] H. J. Worner, J. B. Bertrand, D. V. Kartashov, P. B. Corkum, and D. M. Villeneuve, *Nature (London)* **466**, 604 (2010).
  - [5] J. Breidbach and L. S. Cederbaum, *Phys. Rev. Lett.* **94**, 033901 (2005).
  - [6] O. Smirnova, S. Patchkovskii, Y. Mairesse, N. Dudovich, and M. Y. Ivanov, *Proc. Natl. Acad. Sci. USA* **106**, 16556 (2009).
  - [7] O. Smirnova and M. Ivanov, *Nat. Phys.* **6**, 159 (2010).
  - [8] S. Haessler, J. Caillat, W. Boutu, C. Giovanetti-Teixeira, T. Ruchon, T. Auguste, Z. Diveki, P. Breger, A. Maquet, B. Carre, R. Taïeb, and P. Salières, *Nat. Phys.* **6**, 200 (2010).
  - [9] S. Ghimire, A. D. DiChiara, E. Sistrunk, P. Agostini, L. F. DiMauro, and D. A. Reis, *Nat. Phys.* **7**, 138 (2011).
  - [10] M. Ivanov and O. Smirnova, *Chem. Phys.* **414**, 3 (2013).
  - [11] F. H. M. Faisal and J. Z. Kamiński, *Phys. Rev. A* **56**, 748 (1997).
  - [12] D. Golde, T. Meier, and S. W. Koch, *Phys. Rev. B* **77**, 075330 (2008).
  - [13] A. F. Kemper, B. Moritz, J. K. Freericks, and T. P. Devereaux, *New J. Phys.* **15**, 023003 (2013).
  - [14] T. Otobe, *J. Appl. Phys.* **111**, 093112 (2012).
  - [15] S. Ghimire, A. D. DiChiara, E. Sistrunk, G. Ndabashimiye, U. B. Szafruga, A. Mohammad, P. Agostini, L. F. DiMauro, and D. A. Reis, *Phys. Rev. A* **85**, 043836 (2012).
  - [16] O. D. Mücke, *Phys. Rev. B* **84**, 081202 (2011).
  - [17] A. Schiffrin, T. Paasch-Colberg, N. Karpowicz, V. Apalkov, D. Gerster, S. Muhlbrandt, M. Korbman, J. Reichert, M. Schultze, S. Holzner, J. V. Barth, R. Kienberger, R. Ernstorfer, V. S. Yakovlev, M. I. Stockman, and F. Krausz, *Nature (London)* **493**, 70 (2013).
  - [18] V. Apalkov and M. I. Stockman, *Phys. Rev. B* **86**, 165118 (2012).
  - [19] M. Korbman, S. Y. Kruchinin, and V. S. Yakovlev, *New J. Phys.* **15**, 013006 (2013).
  - [20] V. E. Gruzdev, *Phys. Rev. B* **75**, 205106 (2007).
  - [21] M. Y. Ivanov, M. Spanner, and O. Smirnova, *J. Mod. Opt.* **52**, 165 (2005).
  - [22] M. Lewenstein, P. Balcou, M. Y. Ivanov, A. L'Huillier, and P. B. Corkum, *Phys. Rev. A* **49**, 2117 (1994).
  - [23] R. Murray, M. Spanner, S. Patchkovskii, and M. Y. Ivanov, *Phys. Rev. Lett.* **106**, 173001 (2011).
  - [24] M. Goano, F. Bertazzi, M. Penna, and E. Bellotti, *J. Appl. Phys.* **102**, 083709 (2007).